Al-Azhar Engineering 16th International Conference

Vol. 19, No. 72, July 2024, 267 - 280

EXPERIMENTAL INVESTIGATION ON MECHANICAL PERFORMANCE OF BASALT FIBER-STEEL COMPOSITE BARS

Yasser M. Mohammad[1*], Abd El-kader A. Haridy[1], Abo El-wafa M. El-Thakeb[2]

[1]Department of Civil Engineering, Faculty of Engineering, Al-Azhar University, Qena, Egypt.

[2]Department of Civil Engineering, Faculty of Engineering, Al-Azhar University, Naser City, Cairo, Egypt.

***Correspondence:** Yasser_mahmoud@azhar.edu.eg

Citation:
Y.M. Mohmmad, A.A. Haridy and A.M. El-Thakeb, " Experimental Investigation on Mechanical Performance of Basalt Fiber-Steel Composite Bars", Journal of Al-Azhar University Engineering Sector, vol. 19, pp. 267 - 280, 2024.

Received: 25 December 2023

Revised: 06 March 2024

Accepted: 16 March 2024

DoI:10.21608/auej.2024.258188.1561

ABSTRACT

Recently, a basalt FRP-steel composite bar has been developed as a new ductile material to overcome the low elastic modulus and the brittle behavior of basalt FRP bars and corrosion of conventional steel bars especially structures exposed to a harsh environment. In this investigation, forty-five locally manufactured specimens were organized into three types of basalt FRP-steel composite bars with different ratios: (a) Basalt FRP hybridized with steel- wires scattered in the core; (b) Basalt FRP hybridized with plain steel rod as the inner core of hybrid bar; (c) Basalt FRP hybridized with ribbed steel bar in the center of the core, in addition to the control specimens made of pure basalt FRP bars. Uniaxial tensile tests were conducted to predict the stress-strain curve and to determine the elastic modulus, yield strength, ultimate strength, and post-yield stiffness of tested bars. Test results indicated considerable improvement in elastic modulus for basalt-wire hybrid composite bars. However, increasing the steel wire to BFRP ratio up to 36% led to a significant increase in modulus of elasticity by 64% and reduced the ultimate strain by 32.7%. Also, results showed that after the yield of the inner core of the basalt fiber-steel (plain or ribbed) composite bars and before the fiber fractures the stress-strain curve presented a bilinear behavior coincided with stable post-yield stiffness and remarkable enhancement in ductility was recorded.

KEYWORDS: Experimental investigation, Mechanical performance, BFRP, Basalt FRP-Steel Composite Bar, Uniaxial tensile tests, Ductility, Post-yield stiffness.

بحث عملي على الأداء الميكانيكي لأسياخ الهجين المكونة من الياف البازلت والحديد

ياسر محمود محمد[1*]، عبد القادر أحمد هريدي[1]، أبو الوفا محمد الثاقب عمر[2]

[1]قسم الهندسة المدنية، كلية الهندسة، جامعة الأزهر، قنا، مصر

[2]قسم الهندسة المدنية، كلية الهندسة، جامعة الأزهر، مدينة نصر، القاهرة، مصر

***البريد الاليكتروني للباحث الرئيسي:** Yasser_mahmoud@azhar.edu.eg

الملخص

ظهرت مؤخرا اسياخ الهجين المكونة من ألياف البازلت والحديد كمادة مطيلة للتغلب على معايير المرونة المنخفض والسلوك القصيف لأسياخ ألياف البازلت وكذلك للتغلب على مشكلة صدأ حديد التسليح وخصوصا المستخدم في تسليح المنشآت المعرضة لظروف بيئية صعبة. في هذا البحث خمسة واربعون عينة من اسياخ الهجين المكونة من الياف البازلت والحديد والتي تم تصنيعهم محلياً بنسب تهجين مختلفة وقسمت الي ثلاثة أنواع مختلفة (أ) أسياخ الياف البازلت والمهجنة بأسلاك الحديد و (ب) أسياخ الياف البازلت المهجنة داخلها بأسياخ حديد ملساء و (ج)

أسياخ الياف البازلت والمهجنة في منتصفها بأسياخ الحديد ذات النتوءات بالإضافة إلي عينة مصنوعة من ألياف البازلت فقط. تم إجراء إختبار الشد المحوري لهذه العينات لرسم منحني الاجهاد والإنفعال بغرض تحديد كلاً من معاير المرونة وإجهاد الخضوع والمقاومة القصوى والجساءة المتولدة بعد الخضوع. وقد أوضحت النتائج تحسناً ملحوظاً في معاير المرونة لأسياخ ألياف البازلت المهجنة بأسلاك الحديد حيث أنه بزيادة نسبة اسلاك الحديد إلي ألياف البازلت حتي 36% يؤدي إلي زيادة ملحوظة في معاير المرونة بنسبة 64% و يقابل ذلك نقص في أقصي إنفعال بنسبة 32.7%. أيضاً أظهرت النتائج بعد حدوث الخضوع لأسياخ الحديد الموجودة في قلب القطاع و قبل إنهيار ألياف البازلت المغلفة لقطاع أسياخ ألياف البازلت المهجنة بأسياخ حديد التسليح الأملس أو ذات النتوءات يسلك منحني الإجهاد و الإنفعال سلوكاً ثنائياً متزامناً مع إستقرار في جساءة ما بعد الخضوع. وكذلك تحسن واضح في الممطولية لهذه لأسياخ.

الكلمات المفتاحية : بحث عملي، الأداء الميكانيكي، ألياف البازلت، لأسياخ الهجين المكونة من ألياف البازلت والحديد، إختبار شد محوري، الممطولية، الجساءة التالية للخضوع.

1. Introduction

Conventional steel bars are commonly utilized as reinforcement for concrete structures due to their high modulus of elasticity, high tensile strength, ductility, and elastoplastic characteristics. However, corrosion of steel bars is considered one of the main factors affecting the durability of reinforced concrete structures especially structures that are vulnerable to highly corrosive and hostile environments, this mostly leads to a reduction in their structural integrity and results in high costly maintenance and repair work to address the corrosion issues [1, 2]. Fiber -reinforced polymer (FRP) is an innovative composite material composed of a polymer matrix reinforced with fibers such as glass, carbon, aramid, or basalt which offers a high strength-to-weight ratio, corrosion resistance, and durability, making it an attractive option used as a reinforcement in concrete members instead of traditional steel bars for construction projects [3, 4]. However, low modulus of elasticity and linear behavior for FRP bars led to brittle failure and large deformations for concrete members reinforced with FRP bars than those reinforced with ordinary steel [5]. To address the shortcomings of steel and FRP materials researchers [6 - 10] have employed both steel and FRP bars as main reinforcement to improve ductility and reduce the deflection of hybrid concrete beams; however, the corrosion of the steel bars persisted. Recently researchers adopted to investigate a new generation of hybrid bars by combining two kinds of materials to overcome steel and FRP defects. FRP-steel wires hybrid bars have been developed and investigated by [11 -13] to improve both modulus of elasticity and absorbed energy compared to FRP bars. Additionally, numerous researchers [14 - 18] proposed and developed a steel-FRP composite bar (SFCB) which consists of steel bars as inner core and outer longitudinal FRP in a pultrusion process. Steel-FRP composite bar (SFCB) exhibits a bilinear stress-strain behavior and significant enhancement in ductility and stable post-yield stiffness were recorded after yielding of inner steel rebar. Concrete beams reinforced with steel-FRP composite bar (SFCB) exhibit considerable improvements in ductility and strength capacity, furthermore stable and larger post-yield stiffness values were recorded compared to the regular RC beams [19 - 23].

This study presents an experimental evaluation for basalt fiber-steel composite bars under uniaxial tensile test taking into consideration parameters including type of hybridization (steel wires, plain round steel bar or ribbed steel bar), diameter of inner core, yield strength of the inner core and ratio of the outer basalt fibers to the inner core and compare results with pure basalt FRP bars.

2. Experimental Program

2.1 Manufacture of Basalt Fiber-Steel Composite Bars

In this study, three types of basalt fiber-steel composite bars were designed and produced in addition to the control group (A) made of pure basalt FRP bars:
Basalt FRP hybridized with steel- wires scattered in the core, which arranged in seven groups (B, C, D, E, F, P, and R)
Basalt FRP hybridized with plain round steel bar as the inner core of hybrid bar organized into five groups (M, N, S, T, and U)
Basalt FRP hybridized with a ribbed steel bar in the center of the core presented into two groups (V and X) as shown in Fig. 1 where each group consists of three specimens with a typical structure.

The basalt fiber-steel composite bars were manually fabricated by authors as follows: (1) Select the basalt fiber yarns with an adequate number to achieve the required diameter then cut FRP yarns to the specific length. (2) Acetone was used to clean and polish the inner core (steel wires or steel bars) to remove any grime or rust from its surface. (3) Implement winding roving around the inner core to prevent relative slide between the inner core and the outer fibers and enhance the interface bond. (4) Install the steel wires or steel bars at the center of the selected FRP yarns then impregnate them in unsaturated polyester resin. (5) apply fixation for one end of the hybrid bar while exerting constant tension force on the opposite side until the rebar keeps its inner core position and forms a circular cross-section. (6) A helical basalt thread was wrapped around the hybrid bar to maintain its circular cross-section and create a ribbed surface, then it was finally heated and solidified by applying high temperature. **Table 1** listed the mechanical properties of the inner core (steel wires and steel rebars).

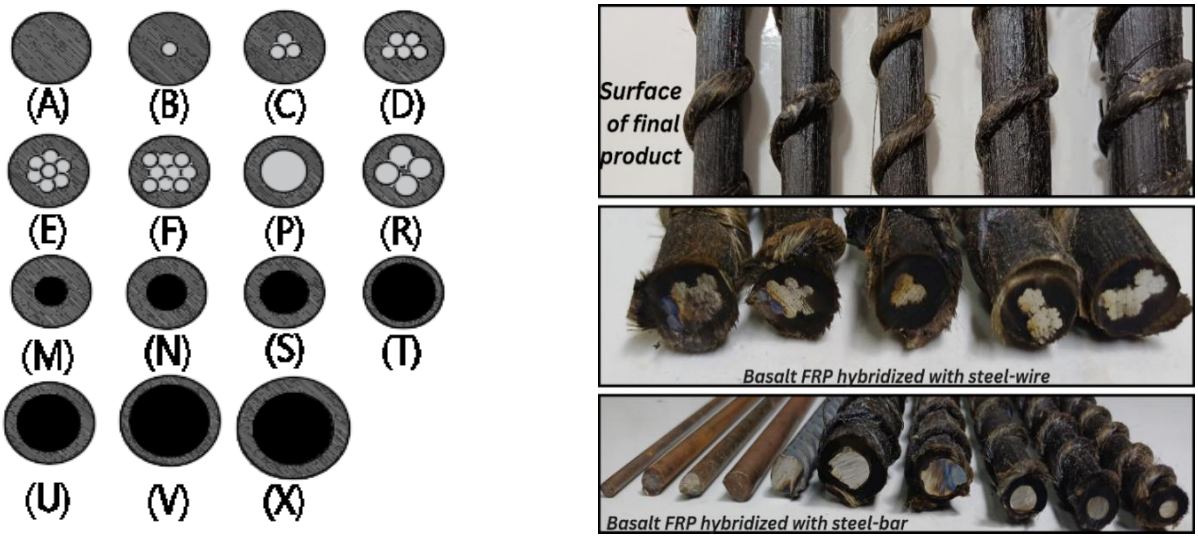

Fig. 1 Cross section type of basalt fiber-steel composite bars.

Table 1. Mechanical properties of inner core (steel wire or steel rebar):

Material	Type	Actual bar diameter (mm)	Yield Strength (MPa)	Ultimate strength (MPa)	Elongation%
Φ 2	Steel wire	1.96	------	1170.9	------
Φ 3	Steel wire	2.94	------	1115	------
Φ 6	Steel wire	5.91	------	1157.2	------
Ø 4	Plain Bar	3.98	420.69	498.39	18.50
Ø 5	Plain Bar	4.96	433.06	507.25	20.10
Ø 6	Plain Bar	6.11	366.08	455.89	26.67
Ø 8	Plain Bar	7.92	382.96	490	22.64
Ø10	Ribbed Bar	10	522.43	692.22	17.93

2.2 Test Instruments

The tested specimens were designed and developed following the guidelines outlined in ASTM D7205M [24]. All specimens had an anchorage system consisting of two steel pipes on both ends of the tested bar filled with an expansive cementitious grout with a length of 300 mm, except specimens arranged in groups U, V, and X, which had an anchor length of 400 mm. As illustrated in Fig. 2 the anchorage system was utilized to distribute uniformly the testing machine stress on the specimens, guarantee specimen failure happens within the tested length, and prevent local failure for the anchor ends of the tested bar.

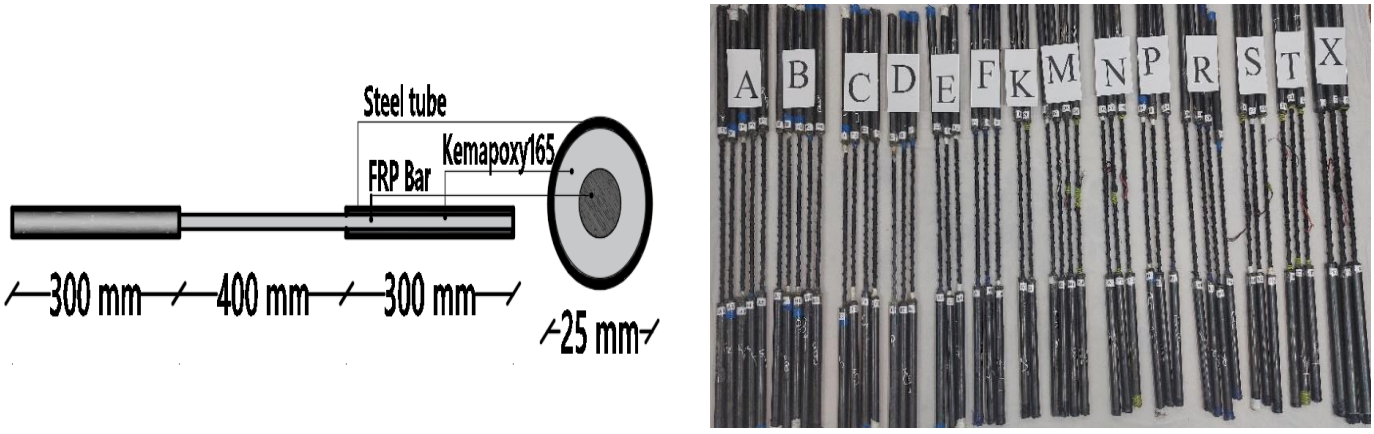

Fig. 2 Dimension of the typical test specimen.

2.3 Uniaxial Tensile Test

The tensile tests were carried out and accomplished using an electrohydraulic universal testing machine with a capacity of 1000 KN under displacement-controlled load with a constant rate of 2.4 mm / min. to determine the stress-strain curve for tested specimens, two linear variable differential transformers (LVDTs) were attached to the tested bar in opposing directions and measure the elongation of the bar within the middle third of its free length by determined the relative longitudinal displacement between the collected readings for LVDTs and divided by the initial length of the bar, as shown in **Fig. 3**.

Fig. 3 Test set-up.

3. Test Results and Discussion

3.1 Basalt Fiber-Steel Wires Composite Bars

Fig. 4 depicts the typical stress-strain curves of basalt fiber-steel wires composite bars with different steel-to-basalt FRP ratios under uniaxial load where, a linear stress-strain relationship was observed for all examined specimens. The equation 1 proposed by the Canadian Standards Association [25] can be used to calculate the modulus of elasticity for a hybrid bar (E_{hybrid}).

$$E_{hybrid} = \frac{(P_1 - P_2)}{(\varepsilon_1 - \varepsilon_2)A_{hybrid}} \quad \text{Eq.1}$$

where, P_1 and P_2 are the applied loads corresponding to 50% and 25% of the ultimate load respectively, while ε_1 and ε_2 are the corresponding strains. A_{hybrid} is a cross-section area for a hybrid bar.

The experimental results of the tested specimens are detailed in **Table 2**. For specimens B, C, D, E, and F, the elastic modulus increased by 0.56, 6.71, 16.27, 31.20, and 62.47 % respectively, when the steel wire to BFRP ratio was increased by 4, 12, 20, 28, and 36% concerning pure BFRP specimens. Conversely, specimens C, D, E, and F exhibited respective reductions by 8.36, 17.87, 22.43, and 32.70% in the ultimate strain ratio as shown in **Fig. 5**. This can significantly improve the characteristics of serviceability by controlling excessive deformations and reducing the width of the crack in the reinforced concrete elements.

Furthermore, as illustrated in **Fig. 6** modifying the diameter of steel wires for the inner core from 9 Ø 2 mm for group F to 4 Ø 3 mm and 1 Ø 6 mm for groups R and P respectively with maintaining the same steel to basalt FRP ratio of 36% had a slight effect on the elastic modulus. Conversely, significant increases in ultimate strain were documented.

Table. 2 Mechanical properties of basalt fiber-steel wires composite bars:

Group	Nominal Diameter A_{sf} (mm)	Inner Core Diameter	Steel-to-BFRP ratio (%)	Modulus of Elasticity E_{hybrid} (GPa)	Ultimate Strength (MPa) f_{sfu}	Ultimate Strain (%) ε_{sfu}
A	10	------	0	47.94	1242.16	2.63
B	10	1 Ø 2 mm	4%	48.21	1232.72	2.66
C	10	3 Ø 2 mm	12%	51.16	1184.68	2.41
D	10	5 Ø 2 mm	20%	55.74	1154.66	2.16
E	10	7 Ø 2 mm	28%	62.9	1230.15	2.04
F	10	9 Ø 2 mm	36%	77.89	1300.5	1.77
P	10	1 Ø 6 mm	36%	72	1233.58	2.12
R	10	4 Ø 3 mm	36%	74.2	1195.84	1.86

The diameter of HBSCB doesn't include the height of deformers or roving winding.

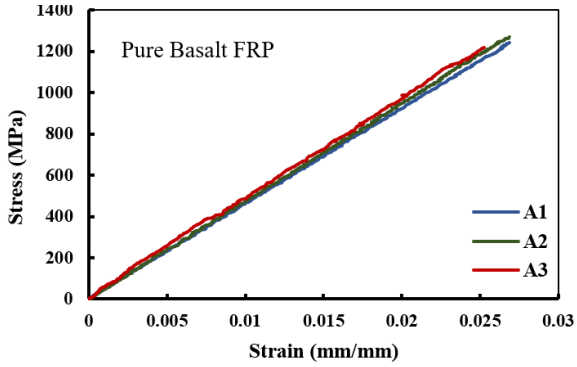

Group A

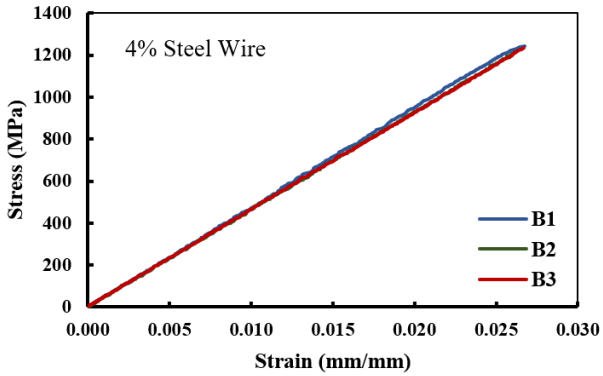

Group B

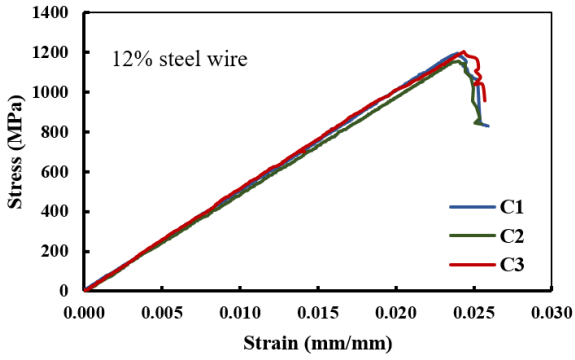

Group C

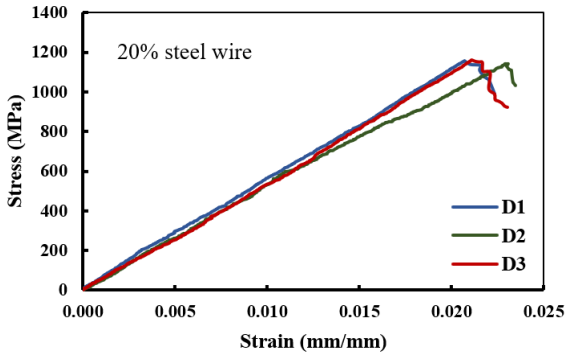

Group D

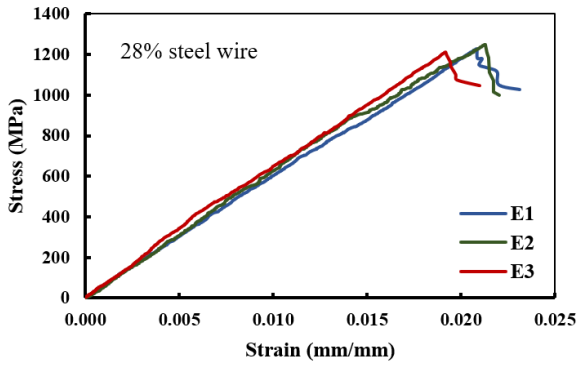

Group E

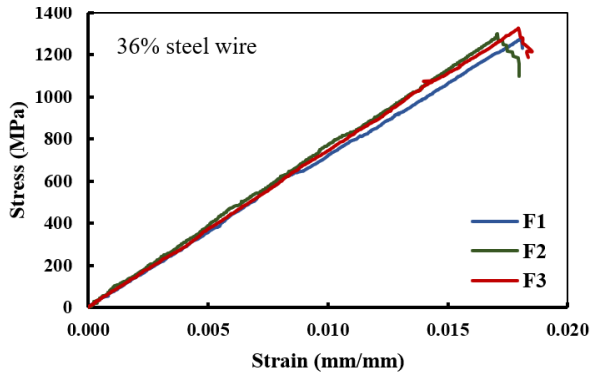

Group F

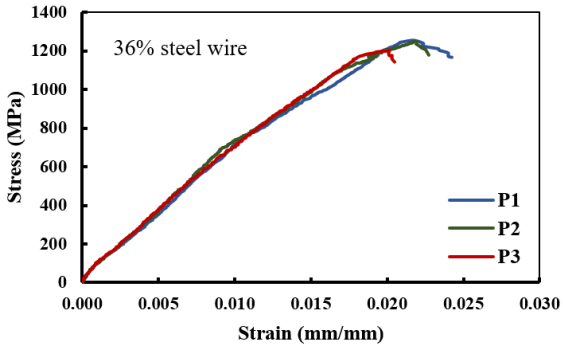

Group P

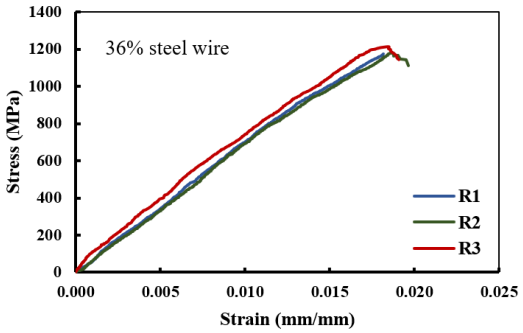

Group R

Fig. 4. Stress-strain curves for basalt fiber-steel wires composite bars.

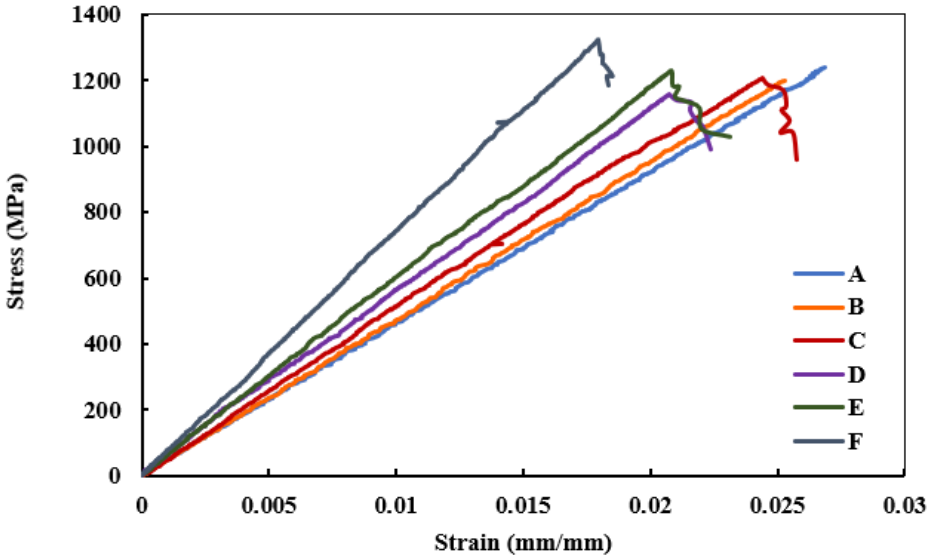

Fig. 5. Comparison between stress-strain curves for groups A, B, C, D, E, and F.

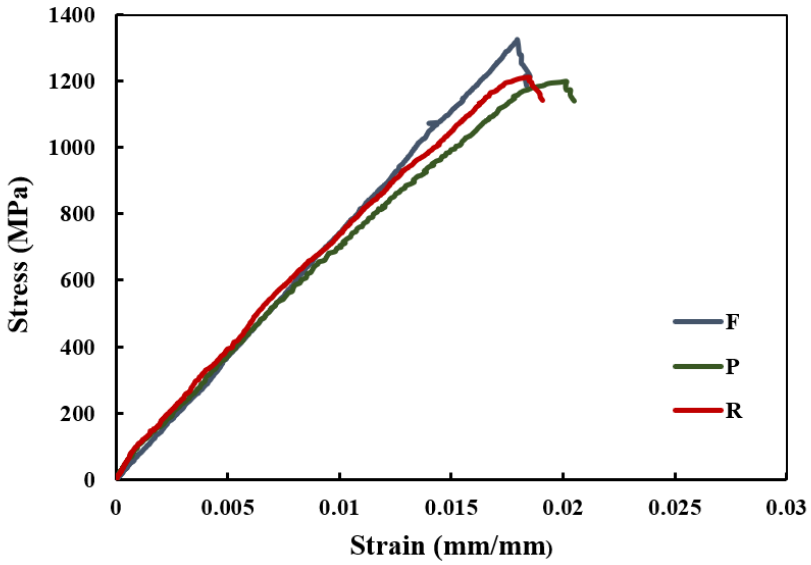

Fig. 6. Comparison between stress-strain curves for groups F, P and R.

3.2. Basalt Fiber-Steel (Plain or Ribbed) Composite Bars

The stress- strain curves for basalt fiber-steel (plain or ribbed) composite bars under monotonic uniaxial load and typical failure mode were Plotted in **Fig. 8**. All tested specimens exhibited a ductile behavior and have a bilinear stress-strain curve in comparison with the linear and brittle manner of basalt FRP bars. At the first stage of loading, both the inner core steel bar and the outer basalt fiber shared the applied load until the inner core steel bar attained its yield strain around 0.002. As the load further increased, the outer basalt fiber effectively carried the load with stable strain increment and the tested specimens exhibited stable post-yield stiffness. Therefore, the load increased, and fracture of the outer basalt fiber occurred when reached its ultimate strain. Subsequently, the load decreased suddenly and was carried by yielded inner core steel until the complete failure took place as shown in **Fig. 7**.

Fig. 7. Mode of failure for basalt fiber-steel (plain and ribbed) composite bars.

The mixture rule can be utilized to forecast the ideal stress-strain relationship of basalt fiber-steel (plain or ribbed) composite bars, provided that a complete bond is established between the outer basalt fiber and the steel inner core [14 - 15].

Table 3 presented experimental properties of basalt fiber-steel (plain and ribbed) composite bars in addition to theoretical calculations according to the following equations [14]:
The strain from zero to yielding of inner steel:

$$\sigma_I = \varepsilon(E_s A_S + E_f A_f)/A \qquad 0 \le \varepsilon \le \varepsilon_y \qquad \text{Eq.2}$$

$$E_I = (E_s A_S + E_f A_f)/A \qquad 0 \le \varepsilon \le \varepsilon_y \qquad \text{Eq.3}$$

The strain from yielding of inner steel to fracture of outside fiber:

$$\sigma_{II} = (E_s A_S + \varepsilon E_f A_f)/A \qquad \varepsilon_y \le \varepsilon \le \varepsilon_{fu} \qquad \text{Eq.4}$$

$$E_{II} = (E_f A_f)/A \qquad \varepsilon_y \le \varepsilon \le \varepsilon_{fu} \qquad \text{Eq.5}$$

The strain from fracture of the outside fibers to inner steel rupture

$$\sigma_{III} = f_y A_S/A \qquad \varepsilon_{fu} \le \varepsilon \le \varepsilon_{s,max} \qquad \text{Eq.6}$$

$$E_{III} = 0 \qquad \varepsilon_{fu} \le \varepsilon \le \varepsilon_{s,max} \qquad \text{Eq.7}$$

Where, E_s and E_f are the modulus of elasticity for steel and BFRP respectively; A_s and A_f are the area of steel inner core and outer basalt fiber respectively; Total basalt fiber-steel (plain or ribbed) composite bars ($A = A_s + A_f$). Also, ε_y is the yielding strain of the inner steel core; ε_{fu} is the fracture strain of outer basalt fiber; $\varepsilon_{(s,max)}$ is the rupture strain for inner steel.

Furthermore , post-yield stiffness r_{sf} can be calculated by the equation 8 suggested by [15, 26]:

$$r_{sf} = \frac{E_f A_f}{(E_s A_s + E_f A_f)} = \frac{E_f A_f}{E_{sf} A_{sf}} \qquad \text{Eq.8}$$

Table 3 indicated that increasing the steel-to-BFRP ratio from 16% to 64% for basalt fiber-plain steel composite bars led to an apparent increase in the initial modulus of elasticity by 192%. Furthermore, significantly decreased the post-yield elasticity by 117%.

Additionally, for basalt fiber-ribbed steel composite bars increasing the steel-to-BFRP ratio from 50% to 64% attributed to obvious increases in initial modulus of elasticity by 105.6%. Moreover, a significant decrease in the post-yield elasticity by 114.1% was observed.

The theoretical results demonstrate a strong correlation with the experimental results for all specimens except a few specific cases. When plain steel was utilized as inner core logical errors were recorded in post-yield modulus E_{II}. Conversely, when the ribbed bars were used as the inner core, there were acceptable deviations in the initial modulus E_I.

Generally, either the manual manufacturing process or the incomplete bonding between the inner core steel and the outer basalt fiber may play a role in these errors.

Table. 3: Mechanical properties of basalt fiber-steel (plain and ribbed) composite bars:

Group	Actual diameter (mm)	Inner Core Diameter	Steel-to-BFRP ratio (%)	Initial Modulus E_I (GPa)			yield Strength f_{sfy} (MPa)			Post-yield Modulus E_{II} (GPa)			Ultimate Strength (MPa)			Post-yield stiffness ratio (r_{sf})
				Exp.	Theo.	Error %	Exp.	Theo.	Error %	Exp.	Theo.	Error %	Exp.	Theo.	Error %	
M	10	1 Ø 4mm[a]	16	83.3	71.24	16.93	187.71	149.6	25.47	40.97	39.55	3.60	875.86	795.53	10	0.96
N	9.85	1 Ø 5mm[a]	25	106.8	85.79	24.49	232.51	180.16	29.05	37.31	35.08	6.35	945.96	906.19	4.39	0.94
S	10.07	1 Ø 6mm[a]	36	99.46	103.37	-3.78	203.16	227.41	-10.66	29.24	29.68	-1.48	866.84	869.25	-0.27	1.01
T	9.94	1 Ø 8mm[a]	64	159.93	144.13	10.96	327.53	288.26	13.62	18.88	17.16	1.00	734.13	649.17	13.1	0.91
U	11.26	1 Ø 8mm[a]	50	128.43	123.2	4.24	287.51	246.4	16.68	22.95	24.25	-5.36	797.6	783.66	1.78	1.03
V	12.49	1 Ø 10mm[b]	64	145.36	145.43	-0.05	326.63	290.86	12.3	25.36	17.23	47.18	734.65	639.36	14.9	0.63
X	14.14	1 Ø 10mm[b]	50	137.64	124	11.00	268.3	248	8.18	30.33	24	26.37	939.34	839.61	11.9	0.75

a: Plain bar; b: Ribbed bar;
The diameter of basalt fiber-steel (plain and ribbed) composite bars. doesn't include the height of deformers or roving winding.

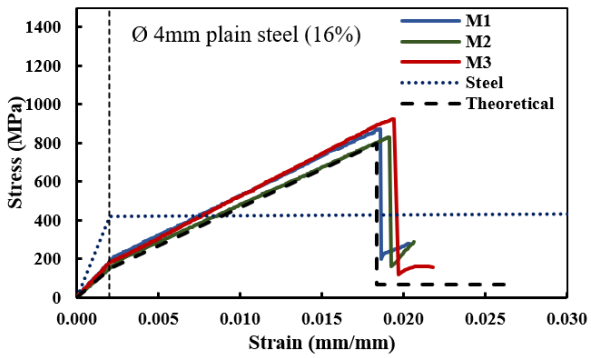

Group M

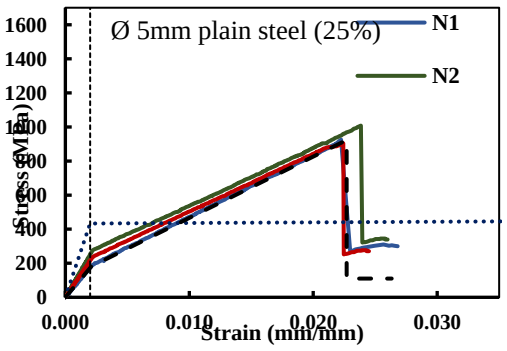

Group N

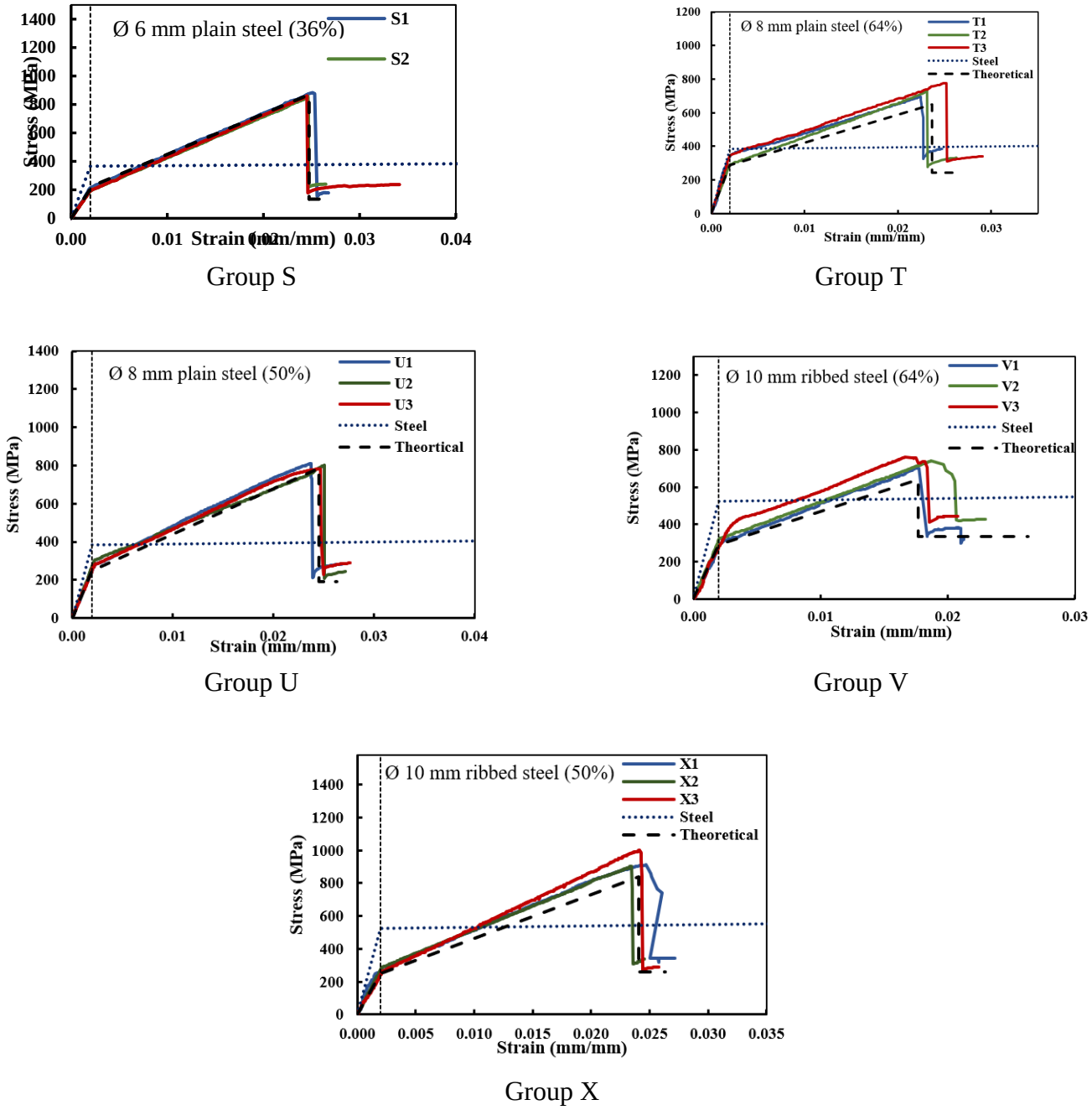

Fig. 8. Comparison between experimental and theoretical stress-strain curves for basalt fiber-steel (plain and ribbed) composite bars.

4. Conclusions

This paper investigated the mechanical properties of locally manufactured Hybrid Basalt Fiber- (Steel wires or steel bar) Composite Bars with different hybridization ratios under uniaxial tensile load. Based on the results obtained in this work, the following conclusions can be drawn:

1- By hybridizing basalt fiber with steel wires, the linear behavior of the stress-strain curve still dominates. However, a considerable enhancement in elastic modulus was recorded.

2- Increasing the steel wire to BFRP ratio for basalt fiber-steel wires composite bars up to 36% led to a significant increase in modulus of elasticity by 64% and reduced ultimate strain by

32.7%, this can substantially enhance the serviceability characteristics of concrete elements by regulating excessive deformations and decreasing the crack width.

3- Employing small-diameter steel wires in the same ratio as an inner core for the basalt fiber-steel wire composite bars resulted in a considerable reduction in their ultimate strain. However, the elastic modulus was very slightly affected.
4- The failure of basalt fiber-steel (plain or ribbed) composite bars under uniaxial tensile load is controlled by fracture of the outer fiber.
5- Basalt fiber-steel (plain or ribbed) composite bars under uniaxial tensile load presented a bilinear stress-strain curve accompanied by stable post-yield stiffness after yielding the inner core.
6- Increasing the steel-to-BFRP ratio from 16% to 64% for basalt fiber-plain steel composite bars led to an obvious increase in the initial modulus of elasticity by 192%. Furthermore, significantly decreases the post-yield elasticity by 117%.
7- Increasing the steel-to-BFRP ratio from 50% to 64% for basalt fiber-ribbed steel composite bars led to a significant increase in initial modulus of elasticity by 105.6%. Furthermore, a remarkable decrease in the post-yield elasticity by 114.1% was recorded.
8- The theoretical model which depends on the mixture rule established a considerable agreement in predicting the stress-strain curves for all specimens of the basalt fiber-steel (plain or ribbed) composite bars except a few specific cases.

Reference

[1] M. Alexander and M. Thomas, “Service life prediction and performance testing - Current developments and practical applications,” *Cem. Concr. Res.*, vol. 78, pp. 155–164, 2015, doi: 10.1016/j.cemconres.2015.05.013.

[2] M. Alexander and H. Beushausen, “Durability, service life prediction, and modelling for reinforced concrete structures – review and critique,” *Cem. Concr. Res.*, vol. 122, no. February, pp. 17–29, 2019, doi: 10.1016/j.cemconres.2019.04.018.

[3] I. F. Kara, A. F. Ashour, and M. A. Köroğlu, “Flexural behavior of hybrid FRP/steel reinforced concrete beams,” *Compos. Struct.*, vol. 129, pp. 111–121, 2015, doi: 10.1016/j.compstruct.2015.03.073.

[4] F. Elgabbas, E. A. Ahmed, and B. Benmokrane, “Flexural Behavior of Concrete Beams Reinforced with Ribbed Basalt-FRP Bars under Static Loads,” *J. Compos. Constr.*, vol. 21, no. 3, 2017, doi: 10.1061/(ASCE)CC.1943-5614.0000752.

[5] T. Ovitigala, M. A. Ibrahim, and M. A. Issa, “Serviceability and ultimate load behavior of concrete beams reinforced with basalt fiber-reinforced polymer bars,” *ACI Struct. J.*, vol. 113, no. 4, pp. 757–768, 2016, doi: 10.14359/51688752.

[6] A. El Refai, F. Abed, and A. Al-Rahmani, “Structural performance and serviceability of concrete beams reinforced with hybrid (GFRP and steel) bars,” *Constr. Build. Mater.*, vol. 96, pp. 518–529, 2015, doi: 10.1016/j.conbuildmat.2015.08.063.

[7] M. Fernand, I. Georges, and M. D. Zakari, “Effect of fiber volume ratio on flexural behavior of RC beam with novel HFRP rebar and steel rebar,” *Structures*, no. March, 2022, doi: 10.1016/j.istruc.2022.06.023.

[8] M. M. Ahmed, A. M. Abdel Hafez, K. A. Assaf, and A. K. Mohamed, “Flexural Behavior of Basalt Frprc Beams Under Repeated Load,” *JES. J. Eng. Sci.*, vol. 42, no. 5, pp. 1179–1192, 2014, doi: 10.21608/jesaun.2014.115060.

[9] A. Hussein, H. Huang, Y. Okuno, and Z. Wu, "Experimental and numerical parametric study on flexural behavior of concrete beams reinforced with hybrid combinations of steel and BFRP bars," *Compos. Struct.*, vol. 302, no. February, p. 116230, 2022, doi: 10.1016/j.compstruct.2022.116230.

[10] Z. Sun, L. Fu, D. C. Feng, A. R. Vatuloka, Y. Wei, and G. Wu, "Experimental study on the flexural behavior of concrete beams reinforced with bundled hybrid steel/FRP bars," *Eng. Struct.*, vol. 197, no. July, p. 109443, 2019, doi: 10.1016/j.engstruct.2019.109443.

[11] D.-W. Seo, K.-T. Park, Y.-J. You, and H.-Y. Kim, "Enhancement in Elastic Modulus of GFRP Bars by Material Hybridization," *Engineering*, vol. 05, no. 11, pp. 865–869, 2013, doi: 10.4236/eng.2013.511105.

[12] X. Wang, Z. Wu, G. Wu, H. Zhu, and F. Zen, "Enhancement of basalt FRP by hybridization for long-span cable-stayed bridge," *Compos. Part B Eng.*, vol. 44, no. 1, pp. 184–192, 2013, doi: 10.1016/j.compositesb.2012.06.001.

[13] T. A. El-Sayed, A. M. Erfan, R. M. Abdelnaby, and M. K. Soliman, "Flexural behavior of HSC beams reinforced by hybrid GFRP bars with steel wires," *Case Stud. Constr. Mater.*, vol. 16, p. e01054, 2022, doi: 10.1016/j.cscm.2022.e01054.

[14] G. Wu, Z.-S. Wu, Y.-B. Luo, Z.-Y. Sun, and X.-Q. Hu, "Mechanical Properties of Steel-FRP Composite Bar under Uniaxial and Cyclic Tensile Loads," *J. Mater. Civ. Eng.*, vol. 22, no. 10, pp. 1056–1066, 2010, doi: 10.1061/(asce)mt.1943-5533.0000110.

[15] G. Wu, Z. Sun, Z. Wu, and Y. Luo, "Mechanical properties of steel-FRP composite bars (SFCBs) and performance of SFCB reinforced concrete structures," *Adv. Struct. Eng.*, vol. 15, no. 4, pp. 625–636, 2012, doi: 10.1260/1369-4332.15.4.625.

[16] Z. Sun, Y. Tang, Y. Luo, G. Wu, and X. He, "Mechanical Properties of Steel-FRP Composite Bars under Tensile and Compressive Loading," *Int. J. Polym. Sci.*, vol. 2017, pp. 1–11, 2017, doi: 10.1155/2017/5691278.

[17] D. Zhao, J. Pan, Y. Zhou, L. Sui, and Z. Ye, "New types of steel-FRP composite bar with round steel bar inner core: Mechanical properties and bonding performances in concrete," *Constr. Build. Mater.*, vol. 242, p. 118062, 2020, doi: 10.1016/j.conbuildmat.2020.118062.

[18] Y. Sun, Z. Sun, L. Yao, Y. Wei, and G. Wu, "Bond performance between SFCBs and grouted sleeves for precast concrete structures," *Adv. Struct. Eng.*, vol. 24, no. 13, pp. 2857–2869, 2021, doi: 10.1177/13694332211001505.

[19] Z. Y. Sun, Y. Yang, W. H. Qin, S. T. Ren, and G. Wu, "Experimental study on flexural behavior of concrete beams reinforced by steel-fiber reinforced polymer composite bars," *J. Reinf. Plast. Compos.*, vol. 31, no. 24, pp. 1737–1745, 2012, doi: 10.1177/0731684412456446.

[20] Y. Yang, Z. Y. Sun, G. Wu, D. F. Cao, and Z. Q. Zhang, "Flexural capacity and design of hybrid FRP-steel-reinforced concrete beams," *Adv. Struct. Eng.*, vol. 23, no. 7, pp. 1290–1304, May 2020, doi: 10.1177/1369433219894236.

[21] Y. Sun, J. Fu, Z. Sun, J. Zhang, Y. Wei, and G. Wu, "Flexural behavior of concrete beams reinforced by partially unbonded steel-FRP composite bars," *Eng. Struct.*, vol. 272, no. August, p. 115050, 2022, doi: 10.1016/j.engstruct.2022.115050.

[22] S. Sun, Y. Guo, P. Gui, L. Xing, and K. Mei, "Flexural behaviour of steel–basalt fiber composite bar-reinforced concrete beams," *Eng. Struct.*, vol. 289, no. April, p. 116246, 2023, doi: 10.1016/j.engstruct.2023.116246.

[23] E. E. Etman, M. H. Mahmoud, A. Hassan, and M. H. Mowafy, "Flexural behaviour of concrete beams reinforced with steel-FRP composite bars," *Structures*, vol. 50, no.

December 2022, pp. 1147–1163, 2023, doi: 10.1016/j.istruc.2023.02.098.

[24] CSA S806-02, "Test method for tensile properties of FRP reinforcement," *Can. Stand. Assoc. Ontario, Canada*, 2002.

[25] CAN/CSA S806-12. (2012). CSA (Canadian Standards Association). Design and construction of building structures with fiber-reinforced polymers (CAN/CSA S806-12). *CAN/CSA S806-12*, *Reaffirmed*.

[26] Z. Sun, Y. Yang, W. Yan, G. Wu, and X. He, "Moment-curvature behaviors of concrete beams singly reinforced by steel-frp composite bars," *Adv. Civ. Eng.*, vol. 2017, 2017, doi: 10.1155/2017/1309629.